LIMNOLOGY
and
OCEANOGRAPHY

ASLO

Limnol. Oceanogr. 61, 2016, 596–609

doi: 10.1002/lno.10235

Factors influencing nitrification rates and the abundance and transcriptional activity of ammonia-oxidizing microorganisms in the dark northeast Pacific Ocean

Jason M. Smith,*[1,2] Julian Damashek,[2] Francisco P. Chavez,[1] Christopher A. Francis[2]
[1]Research Division, Monterey Bay Aquarium Research Institute, Moss Landing, California
[2]Department of Earth System Science, Stanford University, Stanford, California

Abstract

Pelagic marine *Thaumarchaea* play a primary role in ammonia oxidation, an integral part of nitrification and the nitrogen cycle. This study examines how physicochemical and biological variables influence rates of nitrification and the distribution, abundance and activity of ammonia oxidizers throughout the dark northeast Pacific Ocean. Nitrification rates are highest near the epipelagic-upper mesopelagic transition and decrease with depth according to a Martin-like power function, suggestive of a coupling to the organic matter flux. In contrast, archaeal and bacterial ammonia monooxygenase (*amoA*) gene abundance remains fairly constant throughout the upper mesopelagic. Density-based composites reveal nitrification to be highest in the upper pycnocline, within the nitrate:silica and ammonium maxima, while ammonia-oxidizing archaea (AOA) abundances are highest in the lower pycnocline. Water column group A (WCA) and B (WCB) AOA *amoA* genes are present throughout the dark ocean but have no relationship to nitrification rates. WCA comprise the majority of the AOA community above 200 m and WCB comprise the majority of it below 500 m, largely because WCA abundances decrease precipitously from 200 m to 500 m. WCA and WCB *amoA* genes are actively transcribed throughout the dark ocean, irrespective of conditions. Thaumarchaeal urease (*ureC*) genes are also present throughout, implying a widespread capacity for mixotrophy; however, unlike *amoA*, their expression is not detectable. Together, the results support a strong linkage between organic matter flux and nitrification rates, identify density as an important control over AOA distributions, and suggest that WCA and WCB distributions are influenced by the availability of their preferred substrates in the dark ocean.

As the link between nitrogen (N) inputs from the atmosphere by dinitrogen (N_2) fixation and losses by denitrification and anaerobic ammonium oxidation, nitrification plays an important role in the cycling of N in the ocean. The rate at which this process occurs also has an important climate feedback because the ocean supplies $\sim$ 3.6 Tg N yr^{-1} as nitrous oxide (N_2O) (Olivier et al. 1998), a potent greenhouse gas, to the atmosphere, most of which is believed to be produced by nitrification (Freing et al. 2012). Despite these important roles in ocean biogeochemical cycles and global climate, the factors affecting the distribution and rate at which the process occurs in the ocean are not well understood.

As a preferred source of nitrogen to support the growth of plankton (Dortch 1990; Kirchman and Wheeler 1998), ammonium is a valuable but scare resource in the ocean. This is particularly apparent in the vast, dark ocean where 88% of the 6.6×10^5 Tg of fixed nitrogen (N) exists as nitrate (NO_3^-) and only 0.05% as ammonium (Gruber 2008). As physiological data suggests (Martens-Habbena et al. 2009), this is largely because the majority of the ammonium (NH_4^+) liberated during the decomposition of organic matter in the dark ocean is immediately oxidized; first to nitrite (NO_2^-) by ammonia-oxidizing microorganisms and then to nitrate by nitrite-oxidizing microorganisms. Given this point, and the limited evidence of rates being tightly coupled to the flux of organic matter (Ward and Zafiriou 1988; Newell et al. 2011), it seems plausible that the availability of ammonium is an important control over nitrification in the dark ocean.

Another potential factor in determining the magnitude and vertical distribution of nitrification rates in the ocean is

*Correspondence: jsmith@mbari.org

Additional Supporting Information may be found in the online version of this article.

the abundance and activity of the microorganisms that carry out this process, namely the ammonia-oxidizing archaea, for which there is a surplus of evidence to support their primary role in determining rates of nitrification in the ocean (Wuchter et al. 2006; Beman et al. 2008; Newell et al. 2013; Smith et al. 2014b). Originally, all marine AOA were believed to be obligate ammonia oxidizers (Könneke et al. 2005). However, geochemical (Ingalls et al. 2006), physiological (Ouverney and Fuhrman 2000) and genomic evidence (DeLong 2006) now indicate the situation to be more complex. Together, these studies suggest that members of the community maintain several different metabolic strategies, including chemolithoautotrophy linked to ammonia oxidation (Hallam et al. 2006; Ingalls et al. 2006; Santoro et al. 2015) and assimilation of dissolved organic matter (Ouverney and Fuhrman 2000; Herndl et al. 2005), including urea (Alonso-Sáez et al. 2012). However, where and when these different metabolic lifestyles of the pelagic Thaumarchaeota become important remains unclear, despite important implications for our understanding of the factors that regulate the abundance and activity of the AOA, nitrification, and how to best incorporate their role into ocean biogeochemical models.

Identified as unique sequence types in the first survey of archaeal *amoA* genes in the marine environment (Francis et al. 2005), multiple studies now support that water column groups A (WCA) and B (WCB) are distinctive "ecotypes" of the AOA (Hallam et al. 2006; Mincer et al. 2007; Beman et al. 2008; Luo et al. 2014). The WCA or "shallow" ecotype is typically most abundant in the epipelagic and upper mesopelagic (Beman et al. 2008), while the WCB or "deep" ecotype dominates in the meso- and bathypelagic, where the ammonium flux is extremely low (Sintes et al. 2013). Despite their potential importance in the cycling of remineralized nitrogen, there is only limited information available on the abundance of thaumarchaeal ecotypes (Beman et al. 2010; Sintes et al. 2013), and none on their subcellular (transcriptional) activities or the potential contribution of these organisms to nitrification rates in the dark realm of the ocean.

The objective of this study was to examine how physicochemical and biological variables influence rates of nitrification, the abundance of ammonia-oxidizing microorganisms, the abundance and transcriptional activity of the two dominant AOA ecotypes, and how these variables relate to one another throughout the dark realm of the northeast Pacific Ocean. This work was carried out along two repeat hydrography transects through the central California Current System (CCS), an eastern boundary upwelling environment with strong nearshore-to-offshore physical, chemical and biological gradients (Chavez et al. 1991; Collins et al. 2003). As with previous studies in this region, which have primarily focused on characterizing spatiotemporal variability and environmental controls over nitrification and/or ammonia oxidizer community dynamics in the sunlit layer (Ward 2005; Wankel et al. 2007; Santoro et al. 2013; Smith et al. 2014a,b), these gradients allow us to assess how basic environmental variables (density, substrate availability, etc) influence nitrification at subcellular, organismal and biogeochemical scales. Unlike previous studies, we focus primarily on studying nitrification and specific Thaumarchaeota clades in the deeper layers of the central California Current System.

Materials and methods

Samples were collected between 12th July and 22nd July 2010 aboard NOAA Ship MacArthur II, as part of MBARI cruise S310. Hydrographic sampling was conducted at 10 predefined stations (every 20 nautical miles; nmi) starting in Point Reyes, California, U.S.A. and traversing California Cooperative Oceanic Fisheries Investigations (CalCOFI) line 60 from stations 50 to 90, and 10 stations (every 20 nmi) from station 90 to 55 along CalCOFI line 67, terminating in Monterey Bay, California, U.S.A. At each station, sampling and hydrographic profiling were carried out with a conductivity-temperature-depth (CTD) rosette sampler equipped with 12 × 10 L Niskin-type sampling bottles. In addition to the standard CTD measurements, the profiling rosette was equipped with the following sensors: WETstar fluorometer (Wetlabs, Philomath, Oregon, U.S.A.), transmissometer (SeaTech, Bellevue, Washington, U.S.A.), SBE43 dissolved oxygen sensor (Sea-Bird Electronics, Bellevue, Washington, U.S.A.) and a radiometer (Biospherical, San Diego, California, U.S.A.). At each station samples were taken from 12 depths between 0 m and 500 m or 1000 m (0 m, 5 m, 10 m, 20 m, 30 m, 40 m, 60 m, 80 m, 100 m, 150 m, 200 m, 500 m or 1000 m) for determination of chlorophyll (only to 200 m, routinely) and macronutrient concentrations using methodologies described elsewhere (Pennington and Chavez 2000; Collins et al. 2003). Ammonium concentrations were determined fluorometrically (Holmes et al. 1999) while at sea (Smith et al. 2014b).

Determination of ammonia oxidation rates

Rate measurements were conducted using stable isotope tracer additions ($^{15}NH_4^+$) at six depths (30 m, 80 m, 100 m, 150 m, 200 m and 500 m or 1000 m) at four stations: 67–60, 67–90, 60–60, 60–90. Seawater used in all experiments was collected directly from the sampling rosette into 500 mL acid-cleaned brown HDPE bottles. Time zero samples for each bottle were taken following the addition of $^{15}NH_4^+$ (99.7 atom % ^{15}N) to a final label concentration of 200 nmol L^{-1}. Following label addition, bottles were incubated in an on-deck circulating seawater incubator cooled with local surface waters, ranging in temperature from 12°C to 16°C, for 24 h. Subsamples to measure the accumulation of the ^{15}N in the $NO_3^- + NO_2^-$ pool were taken by syringe at 0 h and 24 h, passed through a 0.2 micron filter (Sterivex, Millipore, Massachusetts, U.S.A.) into a 60 mL HDPE vial and frozen at −80°C until analysis. Analyses of the $\delta^{15}N$ in $NO_3^- + NO_2^-$

were performed using the denitrifier method (Sigman et al. 2001) at the University of California Davis Stable Isotope Facility (http://stableisotopefacility.ucdavis.edu/no3.html). The resultant data were used to calculate ^{15}N-based nitrification rates, as described previously (Smith et al. 2014a).

Extraction and processing of nucleic acids from seawater samples

Within 30 min of the sampling rosette arriving on deck, cells were harvested from whole seawater samples by pressure filtration (2 L per depth for RNA or DNA) through 25 mm filters housed in Swinnex filter holders (EMD Millipore, Billerica, Massachusetts, U.S.A.); each sample was first passed through a 10 μm pore size polyester prefilter (EMD Millipore, Billerica, Massachusetts, U.S.A.) and then a 0.2 μm Supor filter (Pall, Port Washington, New York, U.S.A.). The 0.2 μm pore size filters were flash frozen in liquid nitrogen in gasketed 2 mL bead tubes containing a mixture of 0.1 mm and 0.5 mm glass beads. Recent evidence suggests that nitrification does not take place on sinking or suspended particles (Wilson et al. 2014) and that Thaumarchaeota are present at very low abundances on them (relative to the free-living community) (Ganesh et al. 2015). Therefore, 10 μm pore size filters were not analyzed.

DNA was extracted from frozen 0.2 μm pore size filters following the protocol in Lund et al. (2012), with some modifications: 700 mL Sucrose-EDTA lysis buffer (0.75 M sucrose, 20 mM EDTA, 400 mM NaCl and 50 mM Tris) were added prior to agitating the filters for 45 s at speed 5.5 in a FastPrep bead-beating machine (MP Biomedicals, Solon, Ohio, U.S.A.). Then, 100 μL of 10% (weight per volume) sodium dodecyl sulfate and proteinase K (50 mg mL^{-1}) were added, followed by incubation at 55°C overnight. The lysate was purified using the Qiagen Blood & Tissue DNeasy kit (Valencia, California, U.S.A.) following the manufacturer's protocol with an additional wash step with buffer AW2. Purified DNA was quantified using a Qubit fluorometer (Life Technologies, Carlsbad, California, U.S.A.). DNA yields ranged from 0.01 μg L^{-1} to 2.25 μg L^{-1} of seawater across all samples.

RNA was extracted according to the protocol of Church et al. (2005), including modifications outlined elsewhere (Lund et al. 2012). Filter samples were collected and submerged into lysis buffer prior to being flash frozen in liquid nitrogen at sea. At the time of extraction, frozen samples were thawed on ice, after which they were agitated for 45 s at a speed of 5.5 in a FastPrep bead-beating machine (MP Biomedicals, Solon, Ohio, U.S.A.). Samples were then centrifuged for 3 min at 10,000 $\times g$ to pellet filter and cell debris, and the supernatant transferred to a clean microcentrifuge tube. Then, 500 μL of 70% ethanol were added prior to binding and purification of RNA samples using RNeasy columns (Qiagen, Valencia, California, U.S.A.) according to the manufacturer's instructions. Purified RNA was eluted by addition of 50 μL of 95°C DEPC-treated water. An aliquot of the purified RNA was immediately subjected to removal of contaminating DNA using the Turbo DNA-free kit following manufacturer's protocol (Life Technologies, Carlsbad, California).

Complimentary DNA (cDNA) was synthesized using random hexamers and the SuperScript III First-Strand Synthesis System for RT-PCR (Life Technologies, Carlsbad, California, U.S.A.) according to manufacturer's protocol, except for increasing the reverse transcription incubation step to 5 h at 50°C (Lund et al. 2012). Negative reverse transcription control reactions were performed for each sample, replacing the reverse transcriptase enzyme with water.

Quantification of *amoA* genes and mRNA transcripts

Assays for quantification of "total" archaeal *amoA* (AOA) and betaproteobacterial *amoA* (AOB) genes were carried out in 25 μL reactions using SYBR Green chemistry on a StepOne Plus real-time PCR machine (PE Applied Biosystems, Waltham, Massachusetts, U.S.A.), as described previously (Smith et al. 2015). Each reaction contained 12.5 μL Failsafe Green Real-Time PCR PreMix E (Epicentre Biotechnologies, Madison, Wisconsin, U.S.A.), 400 nM each primer, 1.25 U Failsafe Real-Time Enzyme Blend (Epicentre Biotechnologies, Madison, Wisconsin, U.S.A.), and ROX passive reference dye at the concentration recommended by the manufacturer. The betaproteobacterial *amoA* qPCR assay used the amoA1F/2R primer set (Rotthauwe et al. 1997) and the following thermal profile: of 94°C for 3 min followed by 35 cycles of 95°C for 45 s, 56°C for 30 s, 72°C for 50 s, and a plate reading step at 82°C for 10 s. "Total" archaeal *amoA* genes were quantified using the primers Arch-amoAF/Arch-amoAR (Francis et al. 2005) and the following thermal profile: 94°C for 3 min, followed by 35 cycles of 94°C for 30 s, 58°C for 45 s, and 72°C for 50 s, and a plate read at 80°C for 10 s. Average AOA qPCR efficiency was 94%. A melting curve analysis was performed after each SYBR qPCR run with plate reads at a temperature increment of 0.3°C. R^2 values for the standard curves (cycle threshold, C_t, vs. $\log_{10}$ copy number) were 0.98 or better for all runs. Efficiency was calculated relative to a theoretical standard curve slope of 3.32.

The abundance of *amoA* genes related to Water Column A (WCA) and Water Column B (WCB) thaumarchaeal ecotypes was estimated with two independent, non-overlapping qPCR assays (Mosier and Francis 2011). The assays were run with identical reaction chemistries, as follows: 12.5 μL Taqman Environmental Master Mix 2.0 (Life Technologies, Carlsbad, California, U.S.A.), 200 nM of each primer, 300 nM of each probe and either 1 μL DNA or 2 μL cDNA template per reaction (0.5–42 ng template DNA or cDNA per reaction), to a final volume of 25 μL. Cycling conditions were: 95°C for 10 min, 40 cycles of 95°C for 15 s, 56°C for 1 min, followed by detection. All qPCR reactions were run in triplicate with a standard curve spanning approximately 10^0-10^6 templates, run in duplicate. Linearized plasmids containing cloned

inserts of the target gene (TOPO pCR4 vector, Invitrogen) were used as standards. Plasmids were linearized with the restriction enzyme *Not*I (New England Biolabs), purified (DNeasy, Qiagen, San Diego, California, U.S.A.), quantified by fluorometry (Quanti-T HS reagent, Life Technologies, Carlsbad, California, U.S.A.), and stored at −80°C. Fresh standard dilutions were made from frozen stocks for each day of analysis. A minimum of three negative control qPCR reactions, to which no DNA template was added, were analyzed with every assay. Efficiencies for all qPCR assays ranged from 95% to 99% across all samples.

Amplification and sequencing of archaeal *ureC* genes

The distribution and diversity of archaeal *ureC* genes were studied by amplification and sequencing of genes using a PCR reaction chemistry identical to that used for amplification of archaeal *amoA* genes (Smith et al. 2015) and the primer set CRUR_F155 and CRUR_R1420 (Yakimov et al. 2011), which amplifies a 1265 bp fragment. Amplified fragments were cloned using the TOPO TA cloning kit (Life Technologies, Carlsbad, California) and sequenced with an ABI 3100 Capillary Sequencer (Elim Biopharmaceuticals, Hayward, California, U.S.A.). A total of 175 archaeal *ureC*-like sequences were obtained. Sequence alignments were created using the MUSCLE plugin within Geneious 7.1.4 (http://www.geneious.com) (Kearse et al. 2012), using a gap open score of −800. The alignment was manually checked prior to building a neighbor-joining tree using a Jukes-Cantor correction and 1000 neighbor joining bootstrap replicates. UniFrac distances (unweighted) were calculated using the online Fast UniFrac portal (Hamady et al. 2010) and were used as input for non-metric multidimensional scaling analysis (NMDS) using the vegan package in R (Oksanen et al. 2013; R Core Team 2014). Sequences from three bacterial strains were included as an out-group. All *ureC* sequences generated in this study have been deposited in GenBank and are available under accession numbers KR006731-KR006905.

Results

As is evident by the shoaling of the halocline and nitracline from 124 °W (Fig. 1A,B), the cruise traversed upwelling-influenced waters nearshore (stations 55 and 60 on both lines) and then entered the mesotrophic coastal transition zone (station 75 on both lines) (Chavez et al. 1991). The seaward terminus of both transects was the eastern boundary of the California Current jet (station 90 on both lines), evidenced by the low salinity, low nitrate surface waters (Fig. 1A,B). Overall, physicochemical conditions observed during our occupation of lines 60 (Fig. 1B,D,F) and 67 (Fig. 1A,C,E) were highly similar.

The euphotic zone, bounded vertically by the depth of the 1% isolume, deepened along both hydrographic transects, from 27 m to 35 m at upwelling-influenced stations to 45–48 m in the coastal transition zone and 56–58 m in California Current jet. The gradual deepening of the euphotic zone was concurrent with decreases in nitrate (Fig. 1C,D), from 2.9 μM to 3.9 μM nearshore to 0.02 μM to 0.2 μM offshore, and chlorophyll, from 3.9 μg L^{-1} to 13.3 μg L^{-1} and from 0.14 μg L^{-1} to 0.17 μg L^{-1} (Fig. 1E,F contours), concentrations in surface waters. A subsurface chlorophyll maximum (present at all stations) gradually deepened, from $\sim$ 10 m near the coast to $\sim$ 40 m offshore (Fig. 1E,F contours). The primary nitrite maximum was situated just below the subsurface chlorophyll maximum along both transects and varied in intensity from a maximum of 0.75 μmol L^{-1} at 67-60 to a minimum of 0.04 μmol L^{-1} at 67-90 (Fig. 1E,F).

Vertical distributions of "total," WCA and WCB AOA *amoA* genes and mRNA transcripts and β-AOB *amoA* genes were quantified at five depths (30 m, 80 m, 100 m, 150 m, 200 m) at eight stations, extended to 500 m and 1000 m at three stations, and to 2000 m, 3000 m, and 3900 m at two stations. Nitrification rates were measured in the same samples used to quantify *amoA* gene and mRNA transcript abundances at stations 60-60, 60-90, 67-60 and 67-90 at all sampling depths above 1000 m. We chose to analyze and present our data with actual sampling depths normalized to account for the depth of euphotic zone at each station (defined here as the depth of the 1% isolume), to allow for more accurate between-station comparison of remineralization dynamics in the upper mesopelagic zone (Buesseler and Boyd 2009).

Nitrification rates

Nitrification rates ranged from < 0.01 nmol L^{-1} d^{-1} to 90 nmol L^{-1} d^{-1} across all stations/depths (Fig. 2). The depth of highest nitrification activity tended to be at the first interval below the euphotic zone (Fig. 2). Below this depth, rates decreased at all stations to a minimum between 0.4 nmol L^{-1} d^{-1} and 7.1 nmol L^{-1} d^{-1} toward the base of the upper mesopelagic zone (200 m). Below 200 m, rates were detected in samples from 500 m at 67-60 and 60-60 and 1000 m at 67-90 and 60-90, where they were 2 nmol L^{-1} d^{-1} and 5 nmol L^{-1} d^{-1} and 0.7 nmol L^{-1} d^{-1} and 0.8 nmol L^{-1} d^{-1}, respectively. When data from all stations/depths were analyzed together, the equation for the best-fit power law was: rate $= 6.6\left(\frac{x}{100}\right)^{-1.91}$, where x is the rate of nitrification at a depth 100 m below the euphotic zone ($N = 20$, $R^2 = 0.78$, $p < 0.01$).

Distribution of "total," WCA and WCB AOA *amoA* genes with depth

Archaeal *amoA* genes were detected in all samples ($N = 59$) from our study (Fig. 3A). Their abundances ranged from 6×10^3 to 3×10^7 copies L^{-1} over the entire dataset, similar to previous upper water column studies in this region (Mincer et al. 2007; Santoro et al. 2010). AOA *amoA* gene abundances showed a coherent vertical trend at all eight stations: they were highest between $\sim$ 50 m and 200 m (3×10^6 to 4×10^7 copies L^{-1}), decreased 10-fold to 100-fold

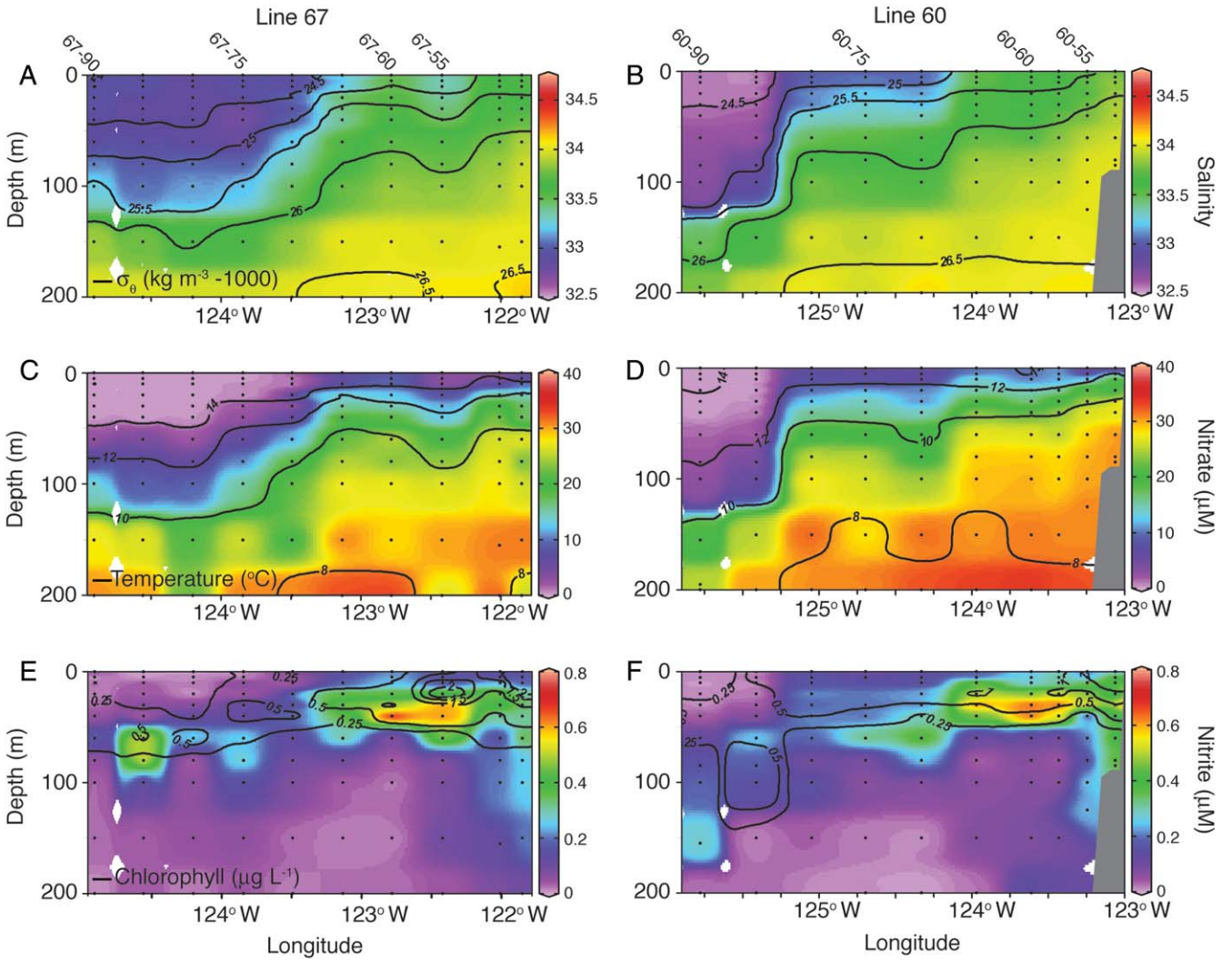

Fig. 1. Salinity (**A**, **B**), nitrate (**C**, **D**) and nitrite (**E**, **F**) in the upper 200 m of the water column along lines 67 (**A**, **C**, **E**) and 60 (**B**, **D**, **F**) extending from the coast of central California into the northeast Pacific Ocean. Density expressed as sigma theta (σ_θ, kg $m^{-3}-1000$) is contoured on salinity panels (**A**, **B**); temperature (°C) is contoured on nitrate panels (**C**, **D**); chlorophyll concentrations (μg L^{-1}) are overlain as contours on the nitrite panels (**E**, **F**). Black dots represent stations/depths where discrete samples were taken for measurement of chlorophyll and macronutrients.

between the mesopelagic and bathypelagic (4×10^5 to 3×10^6 copies L^{-1}) from ~ 500 m to 3000 m below the euphotic zone, and decreased another 10-fold (2×10^5 copies L^{-1}) at the base of the bathypelagic (3900 m) (Fig. 3A).

There were pronounced differences in the vertical distributions of WCA and WCB abundances with depth in the upper mesopelagic. WCA abundances ranged from 2×10^4 to 2×10^7 copies L^{-1} between 0 m and 500 m (Fig. 3B). While they were lowest at station 67-90 and highest at 60-55 at these depths, there was no apparent trend in their abundance with distance from shore along line 60 or 67. There was, however, a coherent vertical trend at 7 of 8 stations. WCA abundances reached a maximum near 50 m at all stations except 67-75 (150 m maximum), below which they initially decreased by 1.5-fold to 6.5-fold down to 200 m ($N = 8$); then, precipitously, by 100-fold, between 200 m and 500 m ($N = 3$). Combined, the WCA abundance data from our stations shows a relatively constant abundance (between 10^6 and 10^7 copies L^{-1}) between the base of the epipelagic (0 m in Fig. 3B) and 200 m, and a steep decline between the upper mesopelagic and interior waters.

WCB *amoA* gene abundances in the upper mesopelagic ranged from 7×10^2 to 2×10^7 copies L^{-1}, and were highest and lowest at 67-70 and 60-90, respectively. WCB *amoA* gene abundances were more variable (vertically) than those of the WCA in the shallow layers of the upper mesopelagic. Unlike the WCA, WCB abundances were highly variable between stations at 50 m and did not reach similar levels at all stations until 100 m. Below this depth their abundances were highly consistent down to 200 m. Overall, the WCA

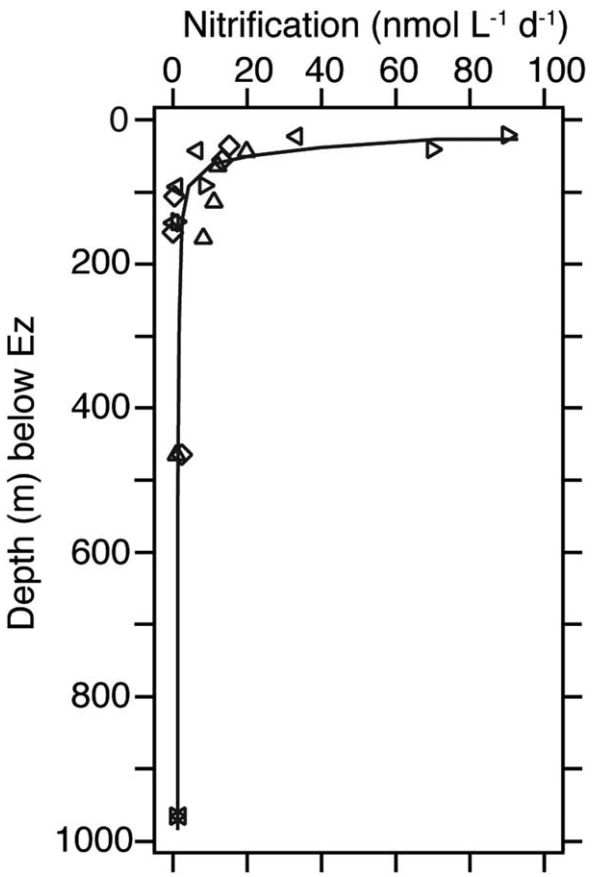

Fig. 2. Nitrification rates determined at stations △**60–60,** ◁**60–90,** ◇**67–60,** ▷**67–90**. To facilitate interpretation of rate data in relation to particle dynamics below the euphotic zone, sampling depths were adjusted to account for depth of the euphotic zone at each station, with a depth of zero being the 1% isolume. The solid line is the line of best fit ($N = 20$, $R^2 = 0.78$, $p < 0.01$) for a power-law function: rate$=6.6\left(\frac{x}{100}\right)^{-1.91}$, where x is the nitrification rate determined at 100 m depth below the euphotic zone.

outnumbered the WCB between 1.5-fold and 680-fold between 0 and 100 m at every station. The WCB outnumbered the WCA by 1.2-fold to 6.5-fold between 100 m and 200 m ($N = 8$) and by 31-fold to 80-fold at 500 m ($N = 3$). The switch from WCA- to WCB-dominated AOA communities was largely driven by steeper rates of decline in the size of the WCA community between 200 m and 500 m below the euphotic zone (Fig. 3B,C).

As in the upper mesopelagic, both WCA and WCB *amoA* genes were present at all interior depths in the ocean, from the top of the mesopelagic (500 m) to the bottom of the bathypelgaic (3900 m). WCA and WCB *amoA* gene abundances ranged from 5×10^1 to 1×10^4 copies L^{-1} and 1×10^4 to 4×10^6 copies L^{-1}, respectively, throughout the interior of the ocean ($N = 12$). WCB became a continually larger fraction of the AOA community with increasing depth in the ocean's interior, outnumbering the WCA by 379-fold to 1465-fold in the lower mesopelagic (750–1000 m, $N = 5$) and 460-fold to 15,000-fold in the bathypelagic (1500–3900 m, $N = 7$) (Fig. 3B,C). The increasing shift toward WCB dominance at depth in the interior ocean was, as in the upper mesopelagic, due to a 2–3 order of magnitude decline in WCA *amoA* gene abundances, while corresponding WCB abundances decreased by only one of order magnitude.

Analysis of our data using density (sigma theta) as a vertical coordinate effectively generated a "composite" of AOA distributions (Fig. 4A–C), chlorophyll concentrations (Fig. 4D), nitrification rates (Fig. 4E) and concentrations of nitrite (Fig. 4F), nitrate relative to silica (NO_3^-: SiO_4^{-4}) (Fig. 4G) and ammonium (Fig. 4H) along the pycnocline in the central CCS. From these data, it became apparent that "total" AOA *amoA* genes (Fig. 4A), as well as those associated with both AOA ecotypes (Fig. 4B,C) are most abundant near the 26.4 kg m^{-3} isopycnal, which occurs substantially deeper in the pycnocline than subsurface maxima in chlorophyll concentrations, nitrification rates, NO_3^-: SiO_4^{-4}, nitrite and ammonium concentrations, which all occurred near 25.5 kg m^{-3} (Fig. 4D–H). Below 26.6 kg m^{-3} ammonium concentrations were consistently below detection (< 5 nmol L^{-1}) (Fig. 4H). The paucity of chlorophyll below 26.5 kg m^{-3} in Fig. 4D reflects the fact that these measurements were not made below 200 m routinely.

Linear regression of AOA *amoA* gene abundances determined using a "general" qPCR assay (Fig. 3A) with the sum of non-overlapping WCA and WCB *amoA* qPCR assays (Fig. 3B,C) suggests that the sum of the ecotype-based assays can be used to estimate the size of the pelagic AOA community as a whole throughout the water column. The parameterized linear regression model for the abundance of "total" AOA *amoA* and WCA+WCB *amoA* genes ($N = 58$, $p < 0.01$, $R^2 = 0.87$) has an intercept of zero and slope (m) of 0.95 ± 0.05 (95% CI) (Supporting Information Fig. S1), which means that "total" AOA *amoA* gene abundances determined using the single assay are 5% higher (on average) than when they are estimated using the sum WCA and WCB *amoA* gene abundances.

Distribution of WCA and WCB *amoA* mRNA transcripts with depth

WCA and WCB *amoA* mRNA transcripts were detected in all samples taken during our study, from the shallow upper mesopelagic to 3900 m, near the seafloor (Fig. 5A,B). WCA and WCB *amoA* mRNA transcripts ranged in abundance from $8 \times 10^{\circ}$ to 6×10^6 copies L^{-1} (Fig. 5A) and $3 \times 10^{\circ}$ to 2×10^5 copies L^{-1} (Fig. 5B), respectively. Transcript abundances were generally more variable between stations than *amoA* genes, particularly for the WCB (Fig. 5B) and showed no relationship with distance from shore. The abundance of both WCA and WCB *amoA* mRNA transcripts followed the same vertical trends observed for their respective genes, as observed for both ecotypes in Monterey Bay (Smith et al. 2014b) and for the AOA community as a whole (Lam et al. 2009; Church et al. 2010). WCA transcripts reached a maximum near 50 m at all stations and decreased slowly down to

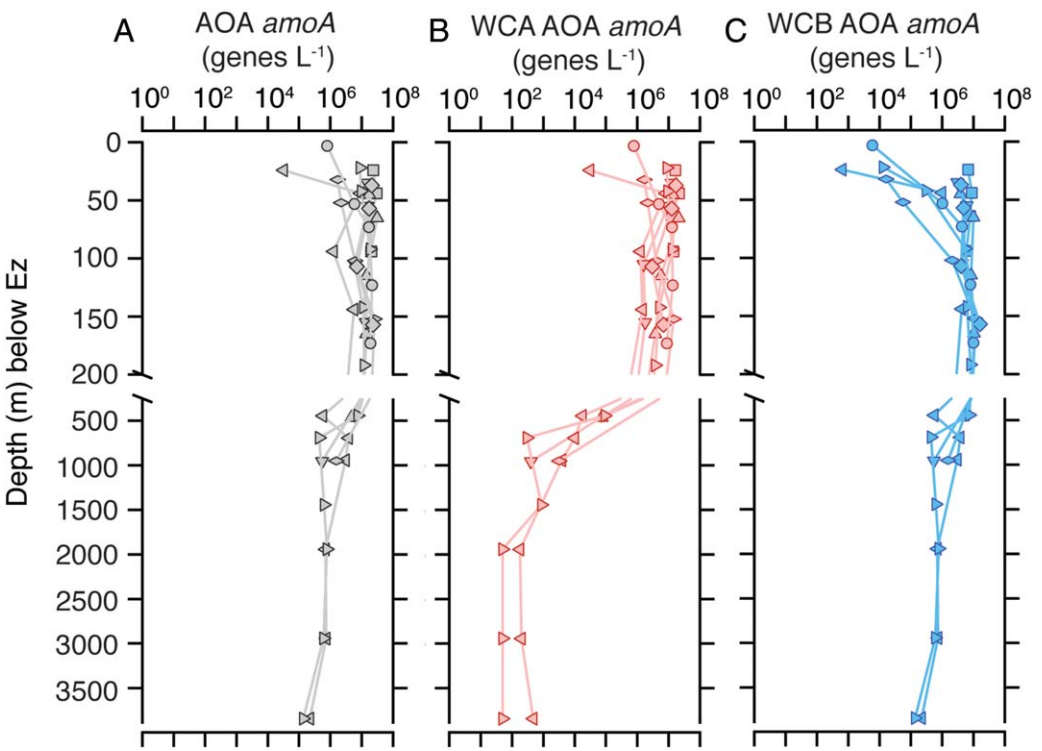

Fig. 3. Abundance of "total" (**A**), WCA (**B**) and WCB (**C**) AOA *amoA* genes at depth below the euphotic zone (Ez) at all stations. To facilitate interpretation of AOA *amoA* gene abundances in relation to particle dynamics below the euphotic zone, sampling depths were adjusted to account for depth of the euphotic zone at each station, with a depth of zero being the 1% isolume. □**60–55,** △**60–60,** ▽**60–75,** ◁**60–90,** ○**67–55,** ◇**67–60,** ◇**67–75,** ▷**67–90**.

500 m before declining precipitously through the interior of the ocean to 3900 m (Fig. 5A). Vertical distributions of WCB transcripts were more variable in magnitude between stations. Like the corresponding *amoA* genes, they showed less vertical variation than those of the WCA at depths in the interior of the ocean (Fig. 5B).

Overall, WCA *amoA* mRNA transcripts consistently outnumbered those of the WCB by 2-fold to 11,000-fold above 200 m in the dark ocean. Below this, WCA transcript abundances decreased quickly down to 1000 m, however WCB transcript abundances were also variable at these depths, causing there to be no consistent trend in abundance; at some stations/depths, WCA transcripts dominated by 3-fold to 48-fold, but at others they were outnumbered 2-fold to 140-fold by the WCB (Fig. 5A,B). Consistency was observed again at interior depths, between 1000 m and 3900 m, where WCB transcripts consistently outnumbered those of the WCA between 1.2-fold and 336-fold (Fig. 5A,B).

No evidence of overexpression of *amoA* mRNA transcripts was found in our dataset (Figs. 3B,C, 5A,B). On average, there were 0.1 (± 0.02; $N = 59$) and 0.014 (± 0.004; $N = 58$) *amoA* mRNA transcripts per gene for the WCA and WCB, respectively. Taking the most basic assumption of one *amoA* gene per genome (Walker et al. 2010; Santoro et al. 2015) and one transcript per active cell (Nakagawa and Stahl 2013), this suggests that 1 of 10 WCA (10%) and 1 of 71 WCB (1.4%) were active at the time of sampling. Combined WCA and WCB data indicates there to be 0.06 transcripts per *amoA* gene, which equates to 1 of 17 AOA cells (5.8%) being active in the dark realm of the ocean.

Diversity of thaumarchaeal *ureC* genes

Genes encoding urease subunit C (*ureC*) in Thaumarchaeota were obtained at stations 67–55, 67–60, 67–90, 60–60, and 60–90, from several depths between 0 m and 3900 m (Fig. 6). Our intention was not to perform an exhaustive survey of marine thaumarchaeal *ureC* diversity, but instead to obtain a broad overview of the lateral and vertical distribution of these genes in the central CCS. Attempts to detect expression of *ureC* mRNA transcripts in our samples were unsuccessful. Thaumarchaeal *ureC* genes from our samples aligned phylogenetically within five of the six previously described marine clades (Yakimov et al. 2011; Alonso-Sáez et al. 2012) (Fig. 6). The majority of sequences grouped into the Marine Clade B.4 (75/175 sequences). While its original description included sequences exclusively from the deep sea (Yakimov et al. 2011), many of our sequences in this clade were from shallower depths, including some from only 80 m, expanding the domain of this clade beyond the bathypelagic. Interestingly, all bathypelagic CCS sequences (from ≥ 2000 m below

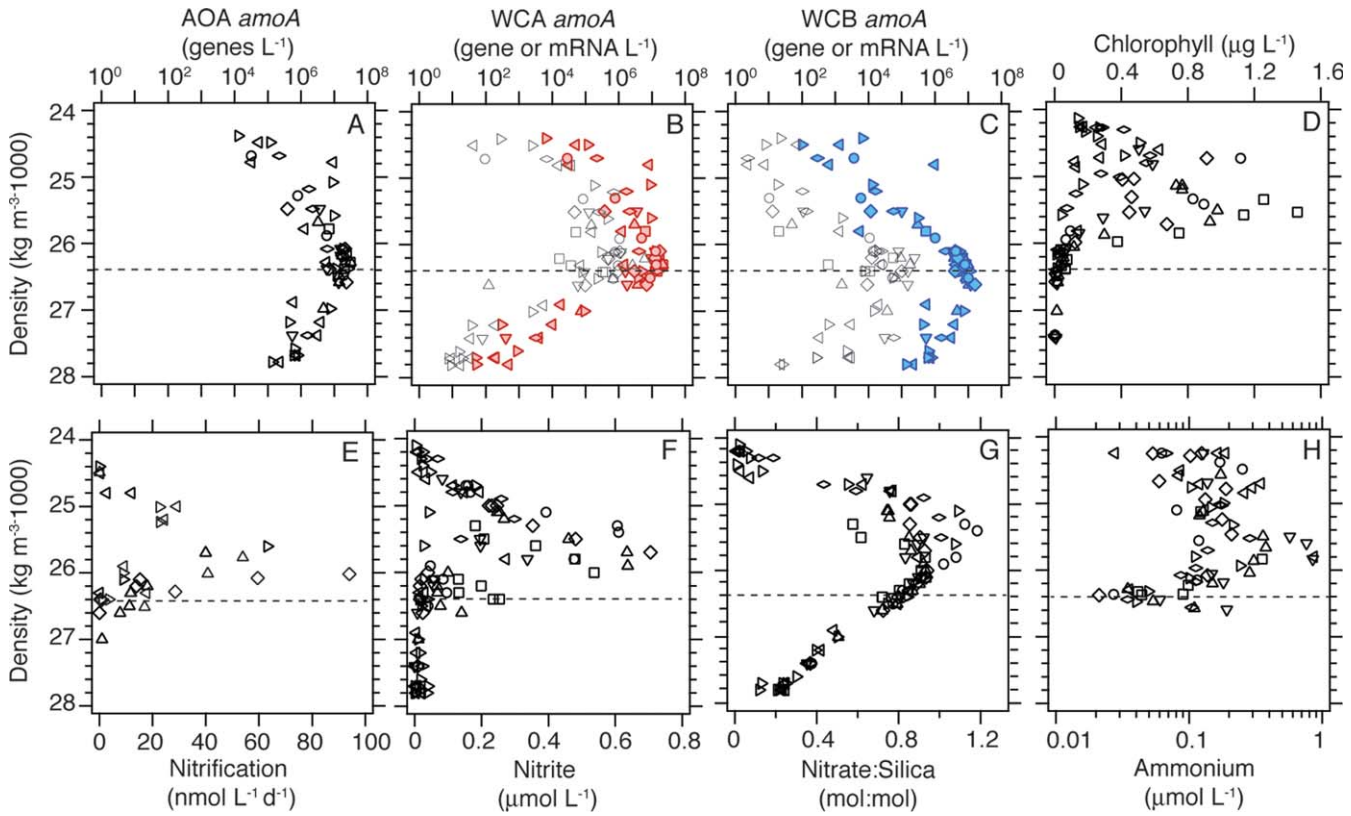

Fig. 4. Density-based composites showing the abundance of (**a**) "total" AOA, (**b**) WCA, (**c**) WCB *amoA* genes, and (**d**) chlorophyll concentrations, (**e**) nitrification rates, and concentrations of (**f**) nitrite, (**g**) nitrate relative to silica (NO_3^-: SiO_4^{-4}) and (**h**) ammonium (note log scale on *x*-axis) along lines 60 and 67. These plots include data from epi-, meso- and bathypelagic depths. Light gray symbols in panels (B) and (C) represent the abundance of *amoA* mRNA transcripts determined in separate samples from the same depth/station. □**60–55,** △**60–60,** ▽**60–75,** ◁**60–90,** ○**67–55,** ◇**67–60,** ◇**67–75**, ▷**67–90**.

the surface) in Marine Clade B.4 grouped in a well-supported branch with a bathypelagic sequence from Station ALOHA (Supporting Information Fig. S2); therefore, specific sub-clades may represent shallow and deep Marine Clade B.4 populations. Like Marine Clade B.4, both shallow and deep CCS sequences grouped in Marine Clade B.2, indicating this clade also does not exclusively represent deep populations (Fig. 6).

In contrast to Marine Clades B.2 and B.4, only CCS sequences from bathypelagic waters grouped in Marine Clade B.1, supporting its designation as a "deep" *ureC* clade. Likewise, the characterization of Marine Clade A.1 as a "shallow" water clade (Yakimov et al. 2011) was supported by our data, as all CCS sequences in this clade were from waters $\leq$200 m below the surface (Fig. 6). A biplot of a UniFrac NMDS analysis suggested little clustering by station, while there was distinct clustering between sequences from shallow ($\leq$ 200 m from the surface) and deep waters (Supporting Information Fig. S3).

Distribution of betaproteobacterial AOB *amoA* genes

Bacterial *amoA* genes were present at concentrations above the limiting threshold of our assays ($\sim$ 10 copies L^{-1}) in 34 of 59 samples. Their genes were only detected in samples from the upper mesopelagic, ranging from 2×10^3 to 7×10^5 genes L^{-1} (Supporting Information Fig. S4). The AOB were between 2 and 3000-fold less abundant than the AOA in our dataset, accounting for $\leq$2% of the ammonia-oxidizing community (AOA+AOB *amoA* genes), which suggests that their role in nitrification is negligible in this environment. For this reason, we did not attempt to quantify β-AOB *amoA* mRNA transcripts as part of this study.

Discussion

Nitrification rates tend to follow a bell curve-like depth distribution in the ocean; rates increase exponentially with depth below the surface to a sometimes narrow (Beman et al. 2012) maximum near the epipelagic-upper mesopelagic boundary, before decreasing to a minimum in the interior ocean (Ward 1987; Ward et al. 1989; Newell et al. 2013). Several lines of geochemical evidence suggest that this vertical distribution could be a response to high rates of organic matter decomposition and remineralization at the base of the euphotic zone (Buesseler et al. 2008, 2009). This idea is well supported in our dataset; most notably by the co-occurrence

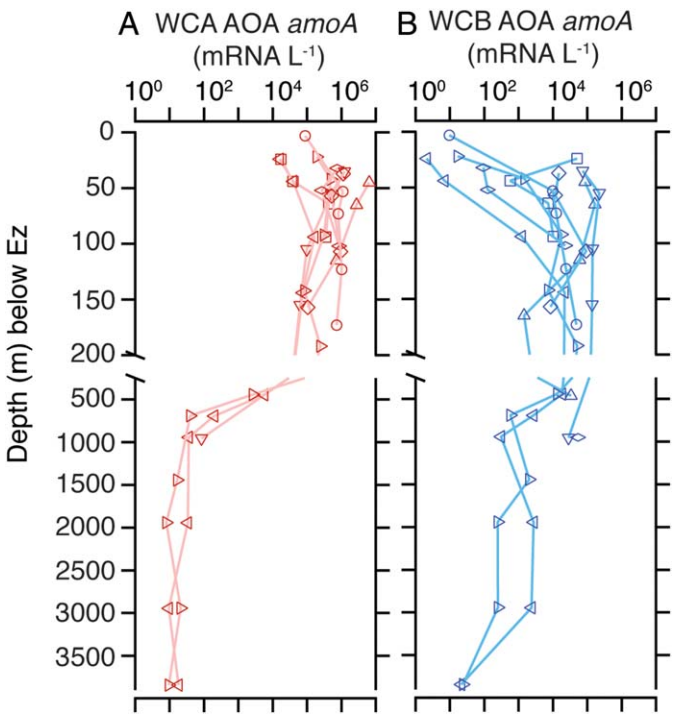

Fig. 5. Depth distributions of WCA (**A**) and WCB (**B**) AOA *amoA* mRNA transcripts at depth below the euphotic zone (Ez) at all stations. To facilitate interpretation of AOA *amoA* gene abundances in relation to particle dynamics below the euphotic zone, sampling depths were adjusted to account for depth of the euphotic zone at each station, with a depth of zero being the 1% isolume. □**60–55,** △**60–60,** ▽**60–75,** ◁**60–90,** ○**67–55,** ◇**67–60,** ◇**67–75,** ▷**67–90**.

of subsurface maxima in ammonium, nitrite and NO_3^-: SiO_4^{-4} concentrations (Fig. 4F–H) just below the chlorophyll maximum (Fig. 4D). Like fixed nitrogen, an important source of silica to the dark ocean is through the biological pump. It has been hypothesized that an excess of nitrate relative to silica is evidence that fixed nitrogen is liberated from organic matter at shallower depths than silica and that the resultant ammonium is oxidized to nitrite and nitrate via nitrification (Buesseler et al. 2008). Therefore, subsurface maxima of nitrite and NO_3^-:SiO_4^{-4} concentrations, in addition to ammonium, may be indicative of high rates of remineralization.

Our data clearly confirm this to be the case in the northeast Pacific Ocean. Nitrification rates (Fig. 4E) are highest at the same position in the pycnocline where the subsurface ammonium (Fig. 4H), nitrite (Fig. 4F) and NO_3^-:SiO_4^{-4} (Fig. 4G) maxima occur, providing the needed biological link between the three geochemical "tracers" of N remineralization. The co-occurrence of these maxima at a specific region in the pycnocline has not been demonstrated previously, and the impacts of this relationship on the use of Si* as tracer of oceanic circulation remain to be determined (Sarmiento et al. 2004). However, the relationship among them is an intuitive one, simply suggesting that the availability of ammonium structures nitrification rates below the euphotic zone. This point is further supported by the fact that they decrease with depth according to a Martin-style power curve (Fig. 2). As with other regions of the ocean (Ward and Zafiriou 1988; Newell et al. 2011), the exponent in the fit equation (0.91), which defines the remineralization path length, is strikingly similar to those determined during several independent sediment trap programs in the region (0.83–0.88) (Martin et al. 1987; Pennington et al. 2010). Together, these data strongly indicate that nitrification rates in the dark realm of the northeast Pacific Ocean are constrained by the organic matter flux, a primary source of ammonium to the dark ocean.

A logical extension of the above observation is to assume that the abundances of the organisms involved in nitrification are also tightly coupled to patterns of N remineralization and the flux of organic matter to depth. As is apparent in the depth profiles from all stations, the abundance of *amoA* genes for both the AOA (Fig. 3A) and *β*-AOB (Supporting Information Fig. S4), as well as both AOA ecotypes (Fig. 3B,C), remain nearly constant in the upper mesopelagic, despite precipitous declines in nitrification rates over this same depth interval (Fig. 2), which is surprising given how tightly coupled they are in the epipelagic (Beman et al. 2008; Smith et al. 2014b).

The vertical distribution of most macronutrients are aligned with the pycnocline in the North Pacific Ocean, meaning the physicochemical environment an organism experiences is likely to be more consistent within a density layer than within a depth horizon (Omand and Mahadevan 2013). The relationship between density and depth is more consistent in permanently stratified regions of the ocean. However, in eastern boundary current systems, such as the central CCS, upwelling causes the pycnocline to shoal nearshore (e.g., Fig. 1A,B), complicating spatiotemporal comparisons along depth strata. In these environments, analysis of data using density and depth can help to resolve the effects of vertical vs. lateral factors on the distribution and activity of microorganisms, and the biogeochemical processes they mediate.

While not apparent in the depth profiles, the density-based composites clearly indicate that AOA *amoA* genes (Fig. 4A) reach their maximum abundance much deeper in the pycnocline than where rates of nitrogen remineralization and nitrification are maximal (Fig. 4E–H). Nitrification rates are highest near the 25.5 kg m^{-3} isopycnal (Fig. 4F), while "total," WCA, and WCB AOA *amoA* genes are most abundant at 26.4 kg m^{-3} (Fig. 4A–C). In our dataset, the 25.5 kg m^{-3} and 26.4 kg m^{-3} isopycnals occur at an average depth of 68 ± 41 m ($N = 20$, range: 21–137 m) and 159 ± 42 m ($N = 20$; range: 112–225 m (Fig. 1A,B), respectively. Put another way, the AOA reach their maximum abundance 91 m deeper than where nitrification and ammonium concentrations are highest (Fig. 4E,H). It is this vertical offset that most strongly suggests there to be additional factors,

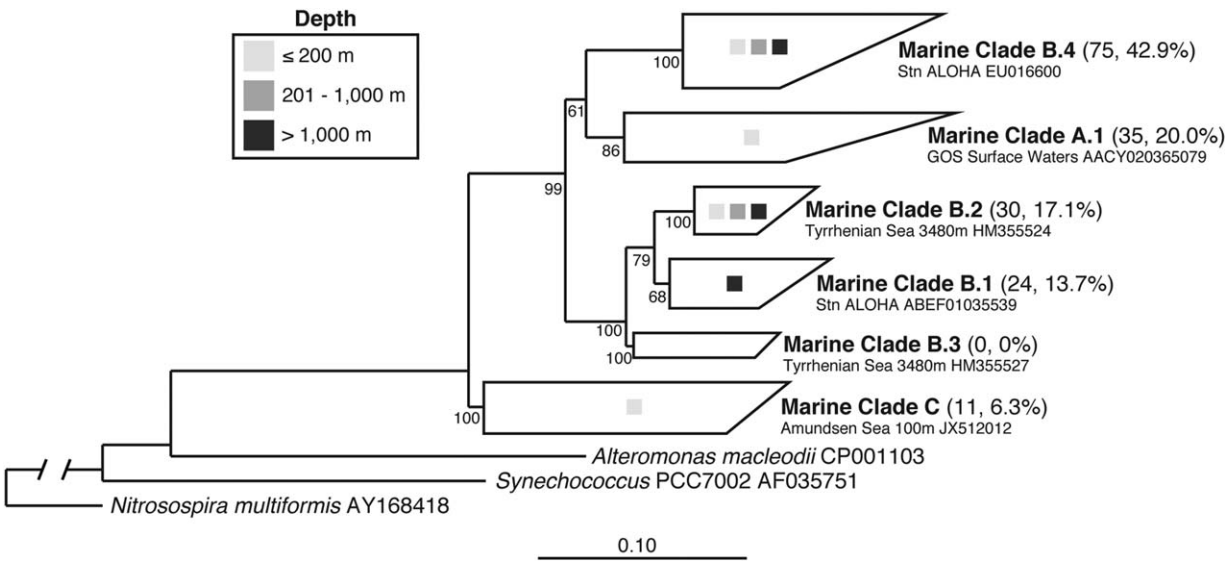

Fig. 6. Neighbor-joining phylogenetic tree of thaumarchaeal *ureC*-like sequences obtained from the central CCS. Major clades are designated and grouped following previously used nomenclature, although the "Polar Marine Clade" named by Alonso-Sáez et al. (2012) has been renamed "Marine Clade C," due to the presence of numerous non-polar sequences within this clade. Parenthetical values give the number of sequences obtained (left) and the percentage of our total sequences (right) in each clade. One reference sequence is indicated next to each clade. Sampling depths of sequences in each clade are designated by shaded squares. Values at nodes indicate bootstrap support (neighbor joining, 1000 replicates).

beyond the availability of ammonium or the supply of organic matter (Fig. 2), that regulate the vertical distribution of ammonia-oxidizing microorganisms in the dark ocean.

Some potential explanations include the possibility that the AOA are able to capture a greater fraction of the ammonium flux, possibly due to there being less bacteria at these depths (Karner et al. 2001), that the community is supported by additional substrates beyond ammonium, such as amino acids (Ouverney and Fuhrman 2000) or urea (Alonso-Sáez et al. 2012), or that rates of vertical mixing and/or predation are reduced in the lower pycnocline. Indeed, repeat hydrography data for the region indicates that the 26.4 kg m^{-3} isopycnal does not outcrop seasonally (Collins et al. 2003) in the central CCS and that it occurs at depths below the winter mixed layer (50–100 m) (Pennington and Chavez 2000), which suggests that physical mixing and stability are important influences on the distribution of AOA *amoA* genes in this region of the ocean.

Presence of Thaumarchaeal urease (*ureC*) genes throughout the dark ocean

One recently put forth idea is that the AOA (or a fraction of them) use urea to support their growth in the ocean (Alonso-Sáez et al. 2012). Whether this reflects different metabolic preferences within the AOA or represents a survival strategy when ammonium is scarce, as it is below 200 m in the northeast Pacific Ocean (Sudek et al. 2015), remains to be determined. The fluxes or sources of urea in the interior of the ocean are also not well understood; presumably it is either excreted by animals or generated during organic matter decomposition (Remsen 1971). In either case, the strength of the source is likely to decrease exponentially with depth below the upper mesopelagic and be very weak below 500 m, where zooplankton biomass is consistently low (Steinberg et al. 2008).

Yet, our sequencing efforts clearly show thaumarchaeal *ureC* genes to be highly diverse and broadly distributed in the central CCS, from upper mesopelagic to bathypelagic depths (down to 3900 m) and from nearshore upwelling-influenced to mesotrophic offshore waters (Fig. 6). Therefore, a fraction of the AOA community throughout this region likely has the ability to use urea. Overall, thaumarchaeal *ureC* diversity appears to be driven primary by depth and not distance from shore (Supporting Information Fig. S3), although some clades include sequences from multiple layers of the water column (Marine Clades B.2. and B.4) while other clades are depth-specific (Marine Clades A.1, B.2, and C; Fig. 6). These data greatly expand existing knowledge of the conditions where thaumarchaeal *ureC* genes occur in the ocean (Hallam et al. 2006; Konstantinidis et al. 2009; Baker et al. 2012; Swan et al. 2014) and indicate the potential for "mixotrophic" growth by the AOA to be widespread in the marine water column. However, our inability to detect *ureC* mRNA transcripts in community RNA suggests that it may not be a dominant thaumarchaeal metabolism in the dark northeast Pacific Ocean.

Distribution, abundance, and activity of WCA and WCB AOA ecotypes

There is a general lack of quantitative information about how the abundance of the two dominant AOA ecotypes vary

with depth in the dark ocean and, until now, none on their transcriptional activity or potential contributions to nitrification in these regions of the marine water column. Depth distributions of WCA and WCB *amoA* genes generally uphold findings observed along a meridional transect in the Atlantic Ocean (Sintes et al. 2013): WCA comprise the majority of the AOA community in the upper 200 m (Fig. 3B), WCB comprise the majority of it at interior depths (Fig. 3C), and the transition between WCA and WCB dominance is largely due to abrupt decreases in WCA abundances between 200 m and 500 m (Fig. 3B,C).

It has been previously hypothesized that these different vertical distributions of the dominant AOA groups in the dark ocean reflect physiological differences in their affinity for ammonium, with the WCA being adapted to the relatively higher ammonium fluxes in the upper mesopelagic zone while WCB are adapted to the very low fluxes characteristic of the interior ocean. Our data coarsely uphold this idea in the upper mesopelagic where there is a surplus of ammonium and the WCA outnumber the WCB (Fig. 3B,C); however, like with the "total" AOA *amoA* genes (discussed above), physical mixing appears to have an important effect on their vertical distributions in the upper mesopelagic (Fig. 4B,C). In the meso- and bathypelagic, the story appears to be a bit more complex.

One explanation for the 2–3 order of magnitude decrease in WCA *amoA* genes between the upper mesopelagic and lower bathypelagic, compared with a 1 order of magnitude decline in the WCB between the same layers (Fig. 3B,C), is that it reflects differences in substrate preferences of WCA and WCB ecotypes. Geochemical evidence from the mesopelagic at station ALOHA indicates the composition of the archaeal community to shift from one comprised of autotrophic ammonia oxidizers (Ingalls et al. 2006; Hansman et al. 2009) to a more heterotrophic (Hansman et al. 2009) one between 600 m and 900 m. The gross flux and lability of organic matter reaching these depths in the north Pacific Ocean is consistently lower in quantity and quality than that of shallower waters (Martin et al. 1987; Buesseler et al. 2007), leading to rapid decreases in the flux of ammonium (Wilson et al. 2014) (Fig. 4F) and other labile nitrogen compounds (McCarthy et al. 1997) in the interior ocean. It seems plausible, then, that the precipitous decrease observed in WCA abundances between 250 m and 1000 m reflects the fact that the majority of them are obligate chemoautotrophic ammonia oxidizers, like the only pelagic marine AOA isolate (Santoro et al. 2015).

In contrast, WCB abundances change very little over this interval but come to comprise > 99% of the AOA community by 1000 m, where radiocarbon data indicate heterotrophy to be the dominant metabolism (Hansman et al. 2009). Similar to the Arabian Sea, there are more AOA (> 99% WCB) at 1000 m than are needed to explain the nitrification rates; rectifying this disparity requires very slow rates of per cell activity and excessively long biomass turnover times (∼ 1500 d) (Newell et al. 2011). Alternatively, this abundance-activity disparity could be explained if the WCB access a wider range of substrates (compared with the WCA) to support their growth and only a fraction of the community oxidizes ammonia.

Great strides have been made using transcriptional data to resolve cellular and biogeochemical complexities in the ocean (Aylward et al. 2015). Unfortunately, the distribution and abundance of WCA and WCB *amoA* mRNA transcripts provides little insight into the factors which influence their respective activities, because they were detected at all depths (Fig. 5A,B). The most striking results of this first effort to quantify the abundance of ecotype-specific AOA *amoA* mRNA transcripts throughout the dark ocean is that the distribution of WCA and WCB transcripts closely mirrors that of their respective *amoA* genes (Figs. 3B,C, 5A,B). In other words, we did not obtain any evidence of transcripts being more abundant than genes ("overexpression"), despite strong ammonium gradients (Fig. 4H) and the decoupling between *amoA* gene abundances (Fig. 5A–C) and nitrification rates (Fig. 5E) in the upper pycnocline. Instead, our data indicate that *amoA* genes associated with both groups are actively transcribed seemingly irrespective of conditions, and suggest that both the WCA and WCB contribute to nitrification throughout the dark ocean. Future work should focus on the potential for metabolic plasticity in AOA communities dominated by the WCB, which have proven difficult to cultivate or study in the laboratory.

References

Alonso-Sáez, L., and others. 2012. Role for urea in nitrification by polar marine Archaea. Proc. Natl. Acad. Sci. USA **109**: 17989–17994. doi:10.1073/pnas.1201914109

Aylward, F. O., J. M. Eppley, J. M. Smith, F. P. Chavez, C. A. Scholin, and E. F. DeLong. 2015. Microbial community transcriptional networks are conserved in three domains at ocean basin scales. Proc. Natl. Acad. Sci. USA **112**: 5443–5448. doi:10.1073/pnas.1502883112

Baker, B. J., R. A. Lesniewski, and G. J. Dick. 2012. Genome-enabled transcriptomics reveals archaeal populations that drive nitrification in a deep-sea hydrothermal plume. ISME J. **6**: 2269–2279. doi:10.1038/ismej.2012.64

Beman, J. M., B. N. Popp, and C. A. Francis. 2008. Molecular and biogeochemical evidence for ammonia oxidation by marine Crenarchaeota in the Gulf of California. ISME J. **2**: 429–441. doi:10.1038/ismej.2007.118

Beman, J. M., R. Sachdeva, and J. A. Fuhrman. 2010. Population ecology of nitrifying Archaea and Bacteria in the Southern California Bight. Environ. Microbiol. **12**: 1282–1292. doi:10.1111/j.1462-2920.2010.02172.x

Beman, J. M., B. N. Popp, and S. E. Alford. 2012. Quantification of ammonia oxidation rates and ammonia-oxidizing

archaea and bacteria at high resolution in the Gulf of California and eastern tropical North Pacific Ocean. Limnol. Oceanogr. **57**: 711–726. doi:10.4319/lo.2012.57.3.0711

Buesseler, K. O., and others. 2007. Revisiting carbon flux through the ocean's twilight zone. Science **316**: 567–570. doi:10.1126/science.1137959

Buesseler, K. O., T. W. Trull, and D. K. Steinberg. 2008. VERTIGO (VERtical Transport In the Global Ocean): A study of particle sources and flux attenuation in the North Pacific. Deep-Sea Res. **55**: 1522–1539. doi:10.1016/j.dsr2.2008.04.024

Buesseler, K. O., and others. 2008. Particle fluxes associated with mesoscale eddies in the Sargasso Sea. Deep-Sea Res. Part II **55**: 1426–1444. doi:10.1016/j.dsr2.2008.02.007

Buesseler, K. O., and P. W. Boyd. 2009. Shedding light on processes that control particle export and flux attenuation in the twilight zone of the open ocean. Limnol. Oceanogr. **54**: 1210–1232. doi:10.4319/lo.2009.54.4.1210

Buesseler, K. O., S. Pike, K. Maiti, C. H. Lamborg, D. A. Siegel, and T. W. Trull. 2009. Thorium-234 as a tracer of spatial, temporal and vertical variability in particle flux in the North Pacific. Deep-Sea Res. Part I **56**: 1143–1167. doi:10.1016/j.dsr.2009.04.001

Chavez, F. P., R. T. Barber, P. M. Kosro, A. Huyer, S. R. Ramp, T. P. Stanton, and B. Rojas de Mendiola. 1991. Horizontal transport and the distribution of nutrients in the coastal transition zone off Northern California: Effects on primary production, phytoplankton biomass and species composition. J. Geophys. Res. **96**: 14833–14848. doi:10.1029/91JC01163

Church, M. J., C. M. Short, B. D. Jenkins, D. M. Karl, and J. P. Zehr. 2005. Temporal patterns of nitrogenase gene (*nifH*) expression in the oligotrophic North Pacific Ocean. Appl. Environ. Microbiol. **71**: 5362–5370. doi:10.1128/AEM.71.9.5362-5370.2005

Church, M. J., B. Wai, D. M. Karl, and E. F. DeLong. 2010. Abundances of crenarchaeal *amoA* genes and transcripts in the Pacific Ocean. Environ. Microbiol. **12**: 679–668. doi:10.1111/j.1462-2920.2009.02108.x

Collins, C. A., J. T. Pennington, C. G. Castro, T. A. Rago, and F. P. Chavez. 2003. The California Current system off Monterey, California: Physical and biological coupling. Deep-Sea Res. Part II **50**: 2389–2404. doi:10.1016/S0967-0645(03)00134-6

DeLong, E. F. 2006. Community genomics among stratified microbial assemblages in the ocean's interior. Science **311**: 496–503. doi:10.1126/science.1120250

Dortch, Q. 1990. The interaction between ammonium and nitrate uptake in phytoplankton. Mar. Ecol. Prog. Ser. **61**: 183–201. doi:10.3354/meps061183

Francis, C. A., K. J. Roberts, J. M. Beman, A. E. Santoro, and B. B. Oakley. 2005. Ubiquity and diversity of ammonia-oxidizing archaea in water columns and sediments of the ocean. Proc. Natl. Acad. Sci. USA **102**: 14683–14688. doi:10.1073/pnas.0506625102

Freing, A., D. W. R. Wallace, and H. W. Bange. 2012. Global oceanic production of nitrous oxide. Philos. Trans. R. Soc. B Biol. Sci. **367**: 1245–1255. doi:10.1098/rstb.2011.0360

Ganesh, S., L. A. Bristow, M. Larsen, N. Sarode, B. Thamdrup, and F. J. Stewart. 2015. Size-fraction partitioning of community gene transcription and nitrogen metabolism in a marine oxygen minimum zone. ISME J. **9**: 2682–2696. doi:10.1038/ismej.2015.44

Gruber, N. 2008. The marine nitrogen cycle: Overview and challenges, p. 1–50. *In* D. G. Capone, D. A. Bronk, M. R. Mulholland and E. J. Carpenter [eds.], Elsevier Inc, Nitrogen in the marine environment.

Hallam, S. J., T. J. Mincer, C. Schleper, C. M. Preston, K. Roberts, P. M. Richardson, and E. F. DeLong. 2006. Pathways of carbon assimilation and ammonia oxidation suggested by environmental genomic analyses of marine Crenarchaeota. PLOS Biol. **4**: e95. doi:10.1371/journal.pbio.0040437

Hamady, M., C. Lozupone, and R. Knight. 2010. Fast UniFrac: Facilitating high-throughput phylogenetic analyses of microbial communities including analysis of pyrosequencing and PhyloChip data. ISME J. **4**: 17–27. doi:10.1038/ismej.2009.97

Hansman, R. L., S. Griffin, J. T. Watson, E. R. M. Druffel, A. E. Ingalls, A. Pearson, and L. I. Aluwihare. 2009. The radiocarbon signature of microorganisms in the mesopelagic ocean. Proc. Natl. Acad. Sci. USA **106**: 6513–6518. doi:10.1073/pnas.0810871106

Herndl, G. J., T. Reinthaler, E. Teira, H. van Aken, C. Veth, A. Pernthaler, and J. Pernthaler. 2005. Contribution of Archaea to total prokaryotic production in the deep Atlantic Ocean. Appl. Environ. Microbiol. **71**: 2303–2309. doi:10.1128/AEM.71.5.2303-2309.2005

Holmes, R. M., A. Aminot, R. Kérouel, B. A. Hooker, and B. J. Peterson. 1999. A simple and precise method for measuring ammonium in marine and freshwater ecosystems. Can. J. Fish. Aquat. Sci. **56**: 1801–1808. doi:10.1139/f99-128

Ingalls, A. E., S. R. Shah, R. L. Hansman, L. I. Aluwihare, G. M. Santos, E. R. M. Druffel, and A. Pearson. 2006. Quantifying archaeal community autotrophy in the mesopelagic ocean using natural radiocarbon. Proc. Natl. Acad. Sci. USA **103**: 6442–6447. doi:10.1073/pnas.0510157103

Karner, M. B., E. F. DeLong, and D. M. Karl. 2001. Archaeal dominance in the mesopelagic zone of the Pacific Ocean. Nature **409**: 507–510. doi:10.1038/35054051

Kearse, M., and others. 2012. Geneious Basic: An integrated and extendable desktop software platform for the organization and analysis of sequence data. Bioinformatics **28**: 1647–1649. doi:10.1093/bioinformatics/bts199

Kirchman, D., and P. A. Wheeler. 1998. Uptake of ammonium and nitrate by heterotrophic bacteria and

phytoplankton in the sub-Arctic Pacific. Deep-Sea Res. Part I **45**: 347–365. doi:10.1016/S0967-0637(97)00075-7

Könneke, M., A. E. Bernhard, J. R. de la Torre, C. B. Walker, J. B. Waterbury, and D. A. Stahl. 2005. Isolation of an autotrophic ammonia-oxidizing marine archaeon. Nature **437**: 543–546. doi:10.1038/nature03911

Konstantinidis, K. T., J. Braff, D. M. Karl, and E. F. DeLong. 2009. Comparative metagenomic analysis of a microbial community residing at a depth of 4,000 meters at station ALOHA in the North Pacific subtropical gyre. Appl. Environ. Microbiol. **75**: 5345–5355. doi:10.1128/AEM.00473-09

Lam, P., and others. 2009. Revising the nitrogen cycle in the Peruvian oxygen minimum zone. Proc. Natl. Acad. Sci. USA **106**: 4752–4757. doi:10.1073/pnas.0812444106

Lund, M. B., J. M. Smith, and C. A. Francis. 2012. Diversity, abundance and expression of nitrite reductase (*nirK*)-like genes in marine thaumarchaea. ISME J. **6**: 1966–1977. doi:10.1038/ismej.2012.40

Luo, H., B. B. Tolar, B. K. Swan, C. L. Zhang, R. Stepanauskas, M. Ann Moran, and J. T. Hollibaugh. 2014. Single-cell genomics shedding light on marine Thaumarchaeota diversification. ISME J. **8**:732–736. doi:10.1038/ismej2013.202

Martens-Habbena, W., P. M. Berube, H. Urakawa, J. R. de la Torre, and D. A. Stahl. 2009. Ammonia oxidation kinetics determine niche separation of nitrifying Archaea and Bacteria. Nature **461**: 976–979. doi:10.1038/nature08465

Martin, J. H., G. A. Knauer, D. M. Karl, and W. W. Broenkow. 1987. VERTEX: Carbon cycling in the northeast Pacific. Deep-Sea Res. Part I **34**: 267–285. doi:10.1016/0198-0149(87)90086-0

McCarthy, M., T. Pratum, J. Hedges, and R. Benner. 1997. Chemical composition of dissolved organic nitrogen in the ocean. Nature **390**: 150–154. doi:10.1038/36535

Mincer, T. J., M. J. Church, L. T. Taylor, C. Preston, D. Karl, and E. F. DeLong. 2007. Quantitative distribution of presumptive archaeal and bacterial nitrifiers in Monterey Bay and the North Pacific subtropical gyre. Environ. Microbiol. **9**: 1162–1175. doi:10.1111/j.1462-2920.2007.01239.x

Mosier, A. C., and C. A. Francis. 2011. Determining the distribution of marine and coastal ammonia-oxidizing archaea and bacteria using a quantitative approach. Method Enzymol. **486**: 206–221. doi:10.1016/B978-0-12-381294-0.00009-2

Nakagawa, T., and D. A. Stahl. 2013. Transcriptional response of the archaeal ammonia oxidizer *Nitrosopumilus maritimus* to low and environmentally relevant ammonia concentrations. Appl. Environ. Microbiol. **79**: 6911–6916. doi:10.1128/AEM.02028-13

Newell, S. E., A. R. Babbin, A. Jayakumar, and B. B. Ward. 2011. Ammonia oxidation rates and nitrification in the Arabian Sea. Global Biogeochem. Cycles **25**: GB4016. doi:10.1029/2010GB003940

Newell, S. E., S. E. Facwett, and B. B. Ward. 2013. Depth distribution of ammonia oxidation rates and ammonia-oxidizer community composition in the Sargasso Sea. Limnol. Oceanogr. **58**: 1491–1500. doi:10.4319/lo.2013.58.4.1491

Oksanen, J., and others. 2013. vegan: Community Ecology Package. R package version 2.0-10. Available from http://CRAN.R-project.org/package=vegan

Olivier, J., K. W. Bouwman, K. W. Van der Hoek, and J. Berdowski. 1998. Global air emission inventories for anthropogenic sources of NO_x, NH_3, and N_2O in 1990. Environ. Pollut. **102**: 135–148. doi:10.1016/S0269-7491(98)80026-2

Omand, M. M., and A. Mahadevan. 2013. Large-scale alignment of oceanic nitrate and density. J. Geophys. Res. Oceans **118**: 5322–5332. doi:10.1002/jgrc.20379

Ouverney, C. C., and J. A. Fuhrman. 2000. Marine planktonic archaea take up amino acids. Appl. Environ. Microbiol. **66**: 4829–4833. doi:10.1128/AEM.66.11.4829-4833.2000

Pennington, J. T., and F. P. Chavez. 2000. Seasonal fluctuations of temperature, salinity, nitrate, chlorophyll and primary production at station H3/M1 over 1989–1996 in Monterey Bay, California. Deep-Sea Res. Part II **47**: 947–973. doi:10.1016/S0967-0645(99)00132-0

Pennington, J. T., G. E. Friederich, C. G. Castro, W. W. Evans, C. A. Collins, and F. P. Chavez. 2010. The northern and central California coastal upwelling system, p. 29–44. *In* K. K. Liu [ed.], Springer-Verlag Berlin Heidelberg, Carbon and nutrient fluxes in continental margins.

R Core Team. 2014. R: A language and environment for statistical computing. R Foundation for Statistical Computing, Vienna, Austria. Available from http://www.R-project.org

Remsen, C. C. 1971. The distribution of urea in coastal and oceanic waters. Limnol. Oceanogr. **16**: 732–740. doi:10.4319/lo.1971.16.5.0732

Rotthauwe, J. H., K. P. Witzel, and W. Liesack. 1997. The ammonia monooxygenase structural gene *amoA* as a functional marker: Molecular fine-scale analysis of natural ammonia-oxidizing populations. Appl. Environ. Microbiol. **63**: 4704–4712.

Santoro, A. E., K. L. Casciotti, and C. A. Francis. 2010. Activity, abundance and diversity of nitrifying archaea and bacteria in the central California Current. Environ. Microbiol. **12**: 1989–2006. doi:10.1111/j.1462-2920.2010.02205.x

Santoro, A. E., and others. 2013. Measurements of nitrite production in and around the primary nitrite maximum in the central California Current. Biogeosciences **10**: 7395–7410. doi:10.5194/bg-10-7395-2013

Santoro, A. E., and others. 2015. Genomic and proteomic characterization of "Candidatus Nitrosopelagicus brevis": An ammonia-oxidizing archaeon from the open ocean.

Proc. Natl. Acad. Sci. USA **112**: 1173–1178. doi:10.1073/pnas.1416223112

Sarmiento, J. L., N. Gruber, M. A. Brzezinski, and J. P. Dunne. 2004. High-latitude controls of thermocline nutrients and low latitude biological productivity. Nature **427**: 56–60. doi:10.1038/nature02127

Sigman, D. M., K. L. Casciotti, M. Andreani, C. Barford, M. Galanter, and J. K. Böhlke. 2001. A bacterial method for the nitrogen isotopic analysis of nitrate in seawater and freshwater. Anal. Chem. **73**: 4145–4153. doi:10.1021/ac010088e

Sintes, E., K. Bergauer, D. De Corte, T. Yokokawa, and G. J. Herndl. 2013. Archaeal *amoA* gene diversity points to distinct biogeography of ammonia-oxidizing *Crenarchaeota* in the ocean. Environ. Microbiol. **15**: 1647–1658. doi:10.1111/j.1462-2920.2012.02801.x

Smith, J. M., F. P. Chavez, and C. A. Francis. 2014a. Ammonium uptake by phytoplankton regulates nitrification in the sunlit ocean. PLoS ONE **9**: e108173. doi:10.1371/journal.pone.0108173

Smith, J., K. L. Casciotti, F. P. Chavez, and C. Francis. 2014b. Differential contributions of archaeal ammonia oxidizer ecotypes to nitrification in coastal surface waters. ISME J. **8**: 1704–1714. doi:10.1038/ismej.2014.11

Smith, J. M., A. C. Mosier, and C. A. Francis. 2015. Spatio-temporal relationships between the abundance, distribution, and potential activities of ammonia-oxidizing and denitrifying microorganisms in intertidal sediments. Microb. Ecol. **69**: 13–24. doi:10.1007/s00248-014-0450-1

Steinberg, D. K., B. Van Mooy, K. O. Buesseler, P. W. Boyd, T. Kobari, and D. M. Karl. 2008. Bacterial vs. zooplankton control of sinking particle flux in the ocean's twilight zone. Limnol. Oceanogr. **53**: 1327–1338. doi:10.4319/lo.2008.53.4.1327

Sudek, S., R. C. Everroad, A.-L. M. Gehman, J. M. Smith, C. L. Poirier, F. P. Chavez, and A. Z. Worden. 2015. Cyanobacterial distributions along a physico-chemical gradient in the Northeastern Pacific Ocean. Environ. Microbiol. **17**: 3692–3707. doi:10.1111/1462-2920.12742

Swan, B. K., and others. 2014. Genomic and metabolic diversity of marine group I Thaumarchaeota in the mesopelagic of the two subtropical gyres. PLoS ONE **9**: e95380. doi:10.1371/journal.pone.0095380

Walker, C. B., and others. 2010. *Nitrosopumilus maritimus* genome reveals unique mechanisms for nitrification and autotrophy in globally distributed marine crenarchaea. Proc. Natl. Acad. Sci. USA **107**: 8818–8823. doi:10.1073/pnas.0913533107

Wankel, S. D., C. Kendall, J. T. Pennington, F. P. Chavez, and A. Paytan. 2007. Nitrification in the euphotic zone as evidenced by nitrate dual isotopic composition: Observations from Monterey Bay, California. Global Biogeochem. Cycles **21**: GB2009. doi:10.1029/2006GB002723

Ward, B. B. 1987. Nitrogen transformations in the Southern California Bight. Deep-Sea Res. Part I **34**: 785–805. doi:10.1016/0198-0149(87)90037-9

Ward, B. B. 2005. Temporal variability in nitrification rates and related biogeochemical factors in Monterey Bay, California, USA. Mar. Ecol. Prog. Ser. **292**: 97–109. doi:10.3354/meps292097

Ward, B. B., and O. C. Zafiriou. 1988. Nitrification and nitric oxide in the oxygen minimum of the eastern tropical North Pacific. Deep-Sea Res. **35**: 1127–1142. doi:10.1016/0198-0149(88)90005-2

Ward, B. B., H. E. Glover, and F. Lipschultz. 1989. Chemoautotrophic activity and nitrification in the oxygen minimum zone off Peru. Deep-Sea Res. Part I **36**: 1031–1051. doi:10.1016/0198-0149(89)90076-9

Wilson, S. T., D. A. del Valle, M. Segura-Noguera, and D. M. Karl. 2014. A role for nitrite in the production of nitrous oxide in the lower euphotic zone of the oligotrophic North Pacific Ocean. Deep-Sea Res. Part I **85**: 47–55. doi:10.1016/j.dsr.2013.11.008

Wuchter, C., and others. 2006. Archaeal nitrification in the ocean. Proc. Natl. Acad. Sci. USA **103**: 12317–12322. doi:10.1073/pnas.0600756103

Yakimov, M. M., and others. 2011. Contribution of crenarchaeal autotrophic ammonia oxidizers to the dark primary production in Tyrrhenian deep waters (Central Mediterranean Sea). ISME J. **5**: 945–961. doi:10.1038/ismej.2010.197

Acknowledgments

The captain and crew of NOAA Ship MacArthur II are thanked for safe and professional facilitation of our work at sea. Holly Gressley is thanked for valuable advice on data presentation. This work was supported in part by the National Science Foundation Grants OCE-0825363 (C.A.F.). Salary support for J. Smith came from the Northern California chapter of the ARCS Foundation, via a graduate research fellowship, and the David and Lucile Packard Foundation, via an MBARI Postdoctoral Fellowship. F. Chavez is also supported by funds provided to MBARI by the David and Lucile Packard Foundation. Partial salary support for J. Damashek came from a Stanford-USGS Graduate Fellowship. Tim Pennington and Marguerite Blum provided assistance with sampling at sea and nutrient analyses. Discussions with Julie Granger, Ryan Paerl and Alyson Santoro and comments from two anonymous reviewers improved this manuscript.

Submitted 14 May 2015
Revised 23 September 2015
Accepted 2 November 2015

Associate editor: Anya Waite